

A Direct Comparison of Reactivity and Mechanism in the Gas Phase and in Solution

John M. Garver,[†] Yao-ren Fang,[‡] Nicole Eyet,^{†,§} Stephanie M. Villano,[†]
Veronica M. Bierbaum,^{*,†} and Kenneth Charles Westaway^{*,‡}

Department of Chemistry and Biochemistry, University of Colorado, Boulder, Colorado 80309,
and Department of Chemistry and Biochemistry, Laurentian University,
Sudbury Ontario, P3E 2C6, Canada

Received November 5, 2009; E-mail: veronica.bierbaum@colorado.edu; kwestaway@laurentian.ca

Abstract: Direct comparisons of the reactivity and mechanistic pathways for anionic systems in the gas phase and in solution are presented. Rate constants and kinetic isotope effects for the reactions of methyl, ethyl, isopropyl, and *tert*-butyl iodide with cyanide ion in the gas phase, as well as for the reactions of methyl and ethyl iodide with cyanide ion in several solvents, are reported. In addition to measuring the perdeutero kinetic isotope effect (KIE) for each reaction, the secondary α - and β -deuterium KIEs were determined for the ethyl iodide reaction. Comparisons of experimental results with computational transition states, KIEs, and branching fractions are explored to determine how solvent affects these reactions. The KIEs show that the transition state does not change significantly when the solvent is changed from dimethyl sulfoxide/methanol (a protic solvent) to dimethyl sulfoxide (a strongly polar aprotic solvent) to tetrahydrofuran (a slightly polar aprotic solvent) in the ethyl iodide–cyanide ion S_N2 reaction in solution, as the “Solvation Rule for S_N2 Reactions” predicts. However, the Solvation Rule fails the ultimate test of predicting gas phase results, where significantly smaller (more inverse) KIEs indicate the existence of a tighter transition state. This result is primarily attributed to the greater electrostatic forces between the partial negative charges on the iodide and cyanide ions and the partial positive charge on the α carbon in the gas phase transition state. Nevertheless, in evaluating the competition between S_N2 and E2 processes, the mechanistic results for the solution and gas phase reactions are strikingly similar. The reaction of cyanide ion with ethyl iodide occurs exclusively by an S_N2 mechanism in solution and primarily by an S_N2 mechanism in the gas phase; only $\sim 1\%$ of the gas phase reaction is ascribed to an elimination process.

Introduction

The influence of solvent on reactions has intrigued chemists for many years. Ions in the gas phase often react differently than the same ions in solution, where coordinating solvent molecules stabilize charges. These effects are evident in the large differences between reaction rate constants of identical gas and condensed phase reactions,^{1,2} in the reversal of ordering of acidities and basicities in solution versus the gas phase,^{3,4} as well as in the enhanced nucleophilicity of polarizable nucleophiles in solution versus the gas phase.⁵

While gas phase studies allow one to probe the intrinsic reactivity of a molecule, a comparison of these results to solution allows one to directly probe the role of the solvent. For example, Figure 1 shows a potential energy diagram for an S_N2 reaction

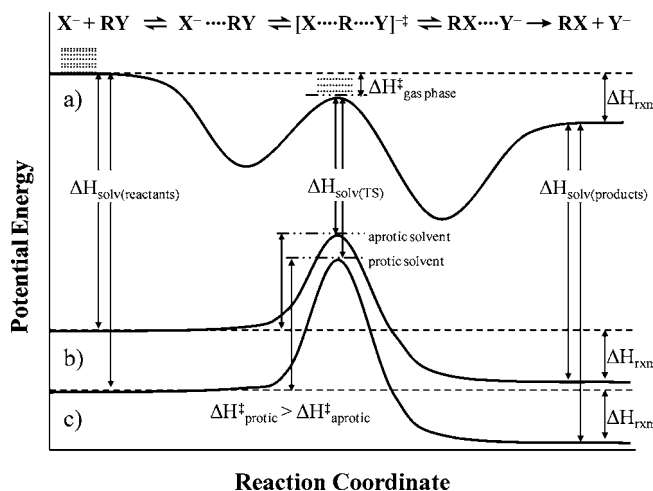


Figure 1. Potential energy diagram of a generic S_N2 reaction in the gas phase (curve a), in an aprotic solvent (curve b), and in a protic solvent (curve c).

in the gas phase (curve a), in an aprotic solvent (curve b), and in a protic solvent (curve c).

In the gas phase, the ion and neutral molecule are attracted by ion-dipole and ion-induced-dipole forces, resulting in the formation of an encounter complex. Because the energy

[†] University of Colorado.

[‡] Laurentian University.

[§] Current address: Department of Chemistry, Saint Anselm College, 100 Saint Anselm Dr. #1760, Manchester, NH 03102.

(1) Bohme, D. K.; Mackay, G. I. *J. Am. Chem. Soc.* **1981**, *103*, 978–979.

(2) Bohme, D. K.; Rakshit, A. B.; Mackay, G. L. *J. Am. Chem. Soc.* **1982**, *104*, 1100–1101.

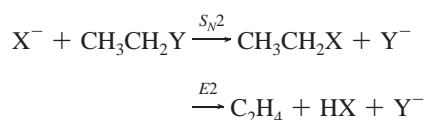
(3) Brauman, J. I.; Blair, L. K. *J. Am. Chem. Soc.* **1970**, *92*, 5986–5987.

(4) Taft, R. W. *Prog. Phys. Org. Chem.* **1983**, *14*, 247–350.

(5) Olmstead, W. N.; Brauman, J. I. *J. Am. Chem. Soc.* **1977**, *99*, 4219–4228.

($\sim 15\text{--}20\text{ kcal mol}^{-1}$)⁶ released in forming the new bonds is converted to internal energy, the complex has sufficient energy to overcome the reaction barrier and form a product complex, which dissociates into the separated products. While there is ample energy for reaction, an ordered transition state slows the process, and hence not every collision results in reaction. The barrier height, and therefore the sum of states above the barrier, can be dramatically different for different ion-neutral pairs. The vertical separation between curves (a) and (b) and between curves (a) and (c) reflects the solvation energy of the reactants, products, and transition state, in the aprotic and protic solvents, respectively. When the reactants and products for the S_N2 reaction in Figure 1 are placed in solution, considerable energy is released due to solvation of the localized charge on the anion and, to a lesser extent, the dipole in the substrate. In the transition state, on the other hand, the charge is dispersed and the solvation energy is much smaller. As a result, the central barrier (ΔH^\ddagger) to reaction is much higher (the reactions are much slower) in solution than in the gas phase; as indicated in Figure 1, reaction barriers are higher in protic solvents relative to aprotic solvents. Figure 1 also defines ΔH^\ddagger for the gas phase transition state relative to the reactants; a more negative ΔH^\ddagger represents a lower energy barrier.

Studies of ion–molecule reactions in both solution and the gas phase have focused on how various nucleophiles, leaving groups, and substituents affect the reactivity of alkyl halides and how various factors determine kinetics, mechanisms, and relative product distributions.^{7–12} In particular, competition between base-induced elimination (E2) and nucleophilic substitution (S_N2) mechanisms is significantly influenced by the nature of the attacking group (X^-), leaving group abilities (Y), substrate properties, and solvent effects.^{13–16}



Substituent effects on transition state structure indicate that both electronic and geometric (steric hindrance) effects influence the $S_N2/E2$ ratio.^{11,17} Condensed and gas phase data show a transition from a predominantly substitution pathway to a predominantly elimination pathway as the steric hindrance around the α -carbon is increased (CH_3CH_2Y to $(CH_3)_2CHY$ to $(CH_3)_3CY$). This shift in reaction pathway occurs because the additional methyl groups increase the steric crowding in the S_N2 transition state, thereby increasing the activation barrier and reducing the reaction rate. In contrast, the activation barrier for the E2 pathway, which is less affected by crowding in the

transition state, appears to be lowered by the additional methyl groups producing faster rates.¹⁷

In previous work, the study of microsolvated ions has been undertaken as a way to bridge the gap between gas phase and solution. Extensive experimental^{18–22} and theoretical^{23–27} work has been carried out to understand S_N2 reactions, while fewer studies have examined E2 reactions.^{28–31} While these experiments have provided valuable insight, they are typically limited to processes with a reaction efficiency greater than 10^{-3} . The direct comparison of gas phase and solution results in this study provides additional insight into this problem.

Deuterium KIEs were employed in our gas and condensed phase reactions to probe the structure of the transition state and relative reaction pathways. A deuterium KIE is the ratio of the rate constant for an undeuterated reactant to the rate constant for a particular deuterated reactant ($KIE = k_H/k_D$). These KIEs are primarily due to changes in the vibrations of bonds involving the isotopes as a reaction proceeds from reactants to products. A normal KIE (>1) is observed when these bonds are loosened on going from reactants to the transition state. This causes a decrease in zero-point energy as the reaction proceeds from separated reactants to the transition state. An inverse KIE (<1) results from the tightening of these bonds on going to the transition state, causing an increase in the difference in zero-point energy as the reaction proceeds. Although normal KIEs are characteristic of E2 reactions and inverse KIEs are typical of S_N2 reactions, this interpretation must be tempered due to minor contributions from all modes (translational, vibrational, rotational). For reactions that proceed by both an E2 and S_N2 mechanism an overall KIE is measured, which provides qualitative insight into the competition between these two mechanisms.

In this study, the reactivity, KIEs, and substituent effects for a series of alkyl iodide–cyanide ion reactions in the gas phase and in solution are evaluated. The reaction rate constants and KIEs for methyl, ethyl, isopropyl, and *tert*-butyl iodide with the cyanide ion in the gas phase, and of methyl and ethyl iodide with the cyanide ion in solution, are reported. The reactions in solution were carried out in three different solvents: a methanol/dimethyl sulfoxide mixture ($CH_3OH/DMSO$), dimethyl sulfoxide (DMSO), and tetrahydrofuran (THF). CH_3OH is a protic solvent that is capable of forming strong hydrogen bonds to the negatively charged nucleophile in the ground state and transition state, DMSO is a very polar aprotic solvent, and THF is a weakly polar aprotic solvent that will solvate ions only very weakly. These solvents provide a smooth gradual transition to

- (6) DePuy, C. H. *J. Org. Chem.* **2002**, *67*, 2393–2401.
- (7) Gronert, S. *Chem. Rev.* **2001**, *101*, 329–360.
- (8) Almerindo, G. I.; Pliego, J. R. *Org. Lett.* **2005**, *7*, 1821–1823.
- (9) Tondo, D. W.; Pliego, J. R. *J. Phys. Chem. A* **2005**, *109*, 507–511.
- (10) Kahn, K.; Bruice, T. C. *J. Phys. Chem. B* **2003**, *107*, 6876–6885.
- (11) Westaway, K. C.; Fang, Y. R.; MacMillar, S.; Matsson, O.; Poirier, R. A.; Islam, S. M. *J. Phys. Chem. A* **2007**, *111*, 8110–8120.
- (12) Westaway, K. C.; Fang, Y. R.; MacMillar, S.; Matsson, O.; Poirier, R. A.; Islam, S. M. *J. Phys. Chem. A* **2008**, *112*, 10264–10273.
- (13) DePuy, C. H.; Gronert, S.; Mullin, A.; Bierbaum, V. M. *J. Am. Chem. Soc.* **1990**, *112*, 8650–8655.
- (14) Uggerud, E. *Pure Appl. Chem.* **2009**, *81*, 709–717.
- (15) Gronert, S. *Acc. Chem. Res.* **2003**, *36*, 848–857.
- (16) Wladkowski, B. D.; Brauman, J. I. *J. Am. Chem. Soc.* **1992**, *114*, 10643–10644.
- (17) Gronert, S.; Fagin, A. E.; Okamoto, K.; Mogali, S.; Pratt, L. M. *J. Am. Chem. Soc.* **2004**, *126*, 12977–12983.

- (18) Bohme, D. K.; Raksit, A. B. *Can. J. Chem.* **1985**, *63*, 3007–3011.
- (19) Kato, S.; Hacialoglu, J.; Davico, G. E.; DePuy, C. H.; Bierbaum, V. M. *J. Phys. Chem. A* **2004**, *108*, 9887–9891.
- (20) O'Hair, R. A. J.; Davico, G. E.; Hacialoglu, J.; Dang, T. T.; DePuy, C. H.; Bierbaum, V. M. *J. Am. Chem. Soc.* **1994**, *116*, 3609–3610.
- (21) Thomas, J. M.; Viggiano, A. A. *J. Phys. Chem. A* **1999**, *103*, 2720–2722.
- (22) Viggiano, A. A.; Arnold, S. T.; Morris, R. A. *Int. Rev. Phys. Chem.* **1998**, *17*, 147–184.
- (23) Davico, G. E. *J. Phys. Chem. A* **2006**, *110*, 13112–13121.
- (24) Hu, W.-P.; Truhlar, D. G. *J. Am. Chem. Soc.* **1994**, *116*, 7797–7800.
- (25) Ohta, K.; Morokuma, K. *J. Phys. Chem.* **1985**, *89*, 5845–5849.
- (26) Tachikawa, H. *J. Phys. Chem. A* **2001**, *105*, 1260–1266.
- (27) Glad, S. S.; Jensen, F. J. *J. Phys. Chem.* **1996**, *100*, 16892–16898.
- (28) Bickelhaupt, F. M.; Baerends, E. J.; Nibbering, N. M. M. *Chem.—Eur. J.* **1996**, *2*, 196–207.
- (29) Eyet, N.; Villano, S. M.; Bierbaum, V. M. *J. Am. Soc. Mass Spectrom.* **2008**, *19*, 1296–1302.
- (30) Eyet, N.; Villano, S. M.; Kato, S.; Bierbaum, V. M. *J. Am. Soc. Mass Spectrom.* **2007**, *18*, 1046–1051.
- (31) Wu, Y.-R.; Hu, W.-P. *J. Am. Chem. Soc.* **1999**, *121*, 10168–10177.

the gas phase conditions. In addition to measuring the perdeutero KIE, $(k_{\text{H}}/k_{\text{D}})_{\text{D}_5}$, for the ethyl iodide reaction, the secondary α -deuterium, $(k_{\text{H}}/k_{\text{D}})_{\alpha\text{-D}_2}$, and secondary β -deuterium, $(k_{\text{H}}/k_{\text{D}})_{\beta\text{-D}_3}$, KIEs were determined for the ethyl iodide reaction. Computational transition states, KIEs, and branching fractions for these reactions provide additional support for our conclusions.

Experimental Section

Gas Phase Experimental. These reactions were carried out in a flowing afterglow-selected ion flow tube (FA-SIFT) mass spectrometer.³² The reactant anion, CN^- , is produced by electron impact on CNBr , mass selected using a quadrupole mass filter, and injected into the reaction flow tube where it becomes thermally equilibrated to room temperature through collisions with He buffer gas (~ 0.5 Torr, $\sim 10^4$ cm s⁻¹). A known flow of neutral reagents was added to the reaction flow tube through a series of fixed inlets at various distances along the flow tube, and the depletion of the reactant ion and formation of the product ions were monitored using the detection quadrupole mass filter coupled to an electron multiplier. Reaction rate constants were determined under pseudo-first-order conditions, where the concentration of the alkyl halide ($\sim 10^{11}$ molecules cm⁻³) was significantly greater than the concentration of the cyanide ion ($\sim 10^5$ ions cm⁻³). The reactant ion signal was monitored as the position of the neutral reagent addition was varied, thereby changing the reaction distance and time. The reaction rate constant is obtained from the slope of a plot of the $\ln[\text{ion}]$ as a function of the neutral reaction distance and other measured experimental parameters. The reported values are the averages of at least three individual measurements.

Absolute uncertainties in these rate measurements are $\pm 20\%$; however some systematic errors (pressure, temperature, He flow rate, etc.) cancel in the rate constant ratio, so that the error bars for KIEs are significantly smaller. Neutral reagents [CH_3I , Aldrich 99.5%; CD_3I , Cambridge Isotope Laboratories 99.5% D; $\text{CH}_3\text{CH}_2\text{I}$, Aldrich 99%; $\text{CD}_3\text{CD}_2\text{I}$, Isotec 99.5% D; $\text{CD}_3\text{CH}_2\text{I}$, Isotec 98% D; $\text{CH}_3\text{CD}_2\text{I}$, Isotec 98% D; $(\text{CH}_3)_2\text{CHI}$, Aldrich 99%; $(\text{CD}_3)_2\text{CDI}$, CDN Isotopes 99.1% D; $(\text{CH}_3)_3\text{CI}$, Aldrich 95%; $(\text{CD}_3)_3\text{CI}$, CDN Isotopes 99.5% D] were obtained from commercial vendors and purified by several freeze–pump–thaw cycles before use. The reagents were protected from light and stored under vacuum. Helium buffer gas (99.995%) was purified by passage through a molecular sieve trap immersed in liquid nitrogen. Parallel reactions of deuterated and undeuterated reactants were carried out under identical conditions.

Condensed Phase Experimental. The rate constants were measured using the procedure outlined for the reaction of ethyl iodide in a previous study,¹² except that the stock solutions were prepared as follows. The alkyl iodide stock solutions for the reactions of ethyl iodide in DMSO and THF were prepared by adding approximately 18 μL of the alkyl iodide to 10 mL of the solvent. For the reaction of ethyl iodide in 90% $\text{CH}_3\text{OH}/10\%$ DMSO (v/v), the ethyl iodide stock solution was prepared by adding 36 μL of ethyl iodide to 10 mL of the solvent. The methyl iodide stock solution for the reaction in 40% $\text{CH}_3\text{OH}/60\%$ DMSO (v/v) was prepared by adding approximately 8 μL of methyl iodide to 10 mL of solvent. The tetrabutylammonium cyanide stock solutions for the ethyl iodide reactions in DMSO and THF and for the methyl iodide reactions in 40% $\text{CH}_3\text{OH}/60\%$ DMSO (v/v) were prepared by dissolving 75 mg of tetrabutylammonium cyanide (accurately weighed) in 50.00 mL of solvent. The tetrabutylammonium cyanide stock solution for the ethyl iodide reaction in 90% $\text{CH}_3\text{OH}/10\%$ DMSO (v/v) was prepared by dissolving approximately 0.170 g of tetrabutylammonium cyanide (accurately weighed) in 25.00 mL of solvent. A 20 mL volume of the tetrabutylammonium cyanide stock solution was transferred into a reaction flask fitted with a serum

cap, and the reaction flask and the alkyl iodide stock solutions were temperature equilibrated for at least 1 h. The reaction was started by injecting 5 mL of the appropriate ethyl iodide stock solution into the reaction flask, and 1.00 mL aliquots of the reaction mixture were taken throughout the reaction and injected into 30 mL of 0.013 M nitric acid. This quenched the reaction by protonating the nucleophile making it unreactive. After the acidic solution containing HCN from the unreacted cyanide ion had been stirred in the fume hood for at least 1 h to remove the hydrogen cyanide, the iodide ion in the sample was analyzed using a potentiometric titration and a 0.0005 M silver nitrate solution. The rate constants were calculated using the standard kinetic equation for a second-order reaction that is first-order in both reactants. The iodide reagents [CH_3I , 99.5%; CD_3I , 99.5% D; $\text{CH}_3\text{CH}_2\text{I}$, 99%; $\text{CD}_3\text{CD}_2\text{I}$, 99.5% D; $\text{CH}_3\text{CD}_2\text{I}$, 98% D] were purchased from Sigma-Aldrich and used without further purification. The reported rate constants are the averages of at least three individual measurements.

Theoretical Calculations. Electronic structure calculations were carried out using the Gaussian 03³³ suite of programs to provide additional insight into the experimental results. Since it has been shown that the calculated KIEs for the ethyl iodide–cyanide ion $\text{S}_{\text{N}}2$ reaction vary markedly with the level of theory,¹² several levels of theory and basis sets were investigated. The MP2³⁴ level of theory with the 6-311++g(2d,p) basis set^{35,36} for C, N, and H and the LanL2DZ effective core potential³⁷ for I correctly predicted the magnitude of the observed $(k_{\text{H}}/k_{\text{D}})_{\alpha\text{-D}_3}$ for the gas phase methyl iodide–cyanide ion reaction, which can only occur by the $\text{S}_{\text{N}}2$ mechanism. Therefore, this level of theory was used in all subsequent calculations and scaling was not applied. Although Scott and Radom have not recommended optimal scaling factors for this level of theory, similar theoretical methods have zero-point vibrational energy, enthalpy, and entropy scaling factors near unity.³⁸ Application of these factors might slightly change the absolute KIE values. However, work on similar reactions by Nielson, Glad, and Jensen indicates scaling does not affect the relative KIEs.³⁹ Therefore, we expect the magnitude and relative changes in our calculated KIEs to provide consistent interpretation of transition structures without scaling. The KIEs were calculated using transition state theory, formulated by assuming that any variational or tunneling effects are insignificant:

$$\frac{k_{\text{H}}}{k_{\text{D}}} = \exp\left(\frac{\Delta G_{\text{D}}^{\ddagger} - \Delta G_{\text{H}}^{\ddagger}}{RT}\right)$$

where $\Delta G^{\ddagger} = G^{\ddagger} - G^{\text{r}}$

ΔG^{\ddagger} is the difference between the zero-point corrected free energy of the transition state relative to the separated reactants. Transition states were confirmed by the existence of one imaginary frequency along the reaction coordinate. The $k_{\text{H}}/k_{\text{D}}$ ratio for the $\text{S}_{\text{N}}2$ and E2 transition states provides relative KIEs for each pathway. The % $\text{S}_{\text{N}}2$ was determined using the same formula with the ratio of the theoretical rate constants for the perprotio reaction, $k_{\text{S}_{\text{N}}2}/(k_{\text{S}_{\text{N}}2} + k_{\text{E}2})$. All frequencies are treated using the harmonic approximation. Although harmonic treatment of low frequency modes can introduce error into the entropy term of the free energy,

(32) Van Doren, J. M.; Barlow, S. E.; DePuy, C. H.; Bierbaum, V. M. *Int. J. Mass Spectrom. Ion Proc.* **1987**, *81*, 85–100.

(33) Frisch, M. J. *Gaussian 03*, revision-B.05; Gaussian Inc.: Pittsburgh, PA, 2004.

(34) Moller, C.; Plesset, M. S. *Phys. Rev.* **1934**, *46*, 618–622.

(35) Zhang, Q. Z.; Wang, H. N.; Sun, T. L.; Wang, W. X. *Chem. Phys.* **2006**, *324*, 298–306.

(36) Hadad, C. M.; Rablen, P. R.; Wiberg, K. B. *J. Org. Chem.* **1998**, *63*, 8668–8681.

(37) Hay, P. J.; Wadt, W. R. *J. Chem. Phys.* **1985**, *82*, 270–283.

(38) Merrick, J. P.; Moran, D.; Radom, L. *J. Phys. Chem. A* **2007**, *111*, 11683–11700.

(39) Nielson, P. A.; Glad, S. S.; Jensen, F. J. *J. Am. Chem. Soc.* **1996**, *118*, 10577–10583.

Table 1. Rate Constants ($10^{-11} \text{ cm}^3 \text{ s}^{-1}$), Reaction Efficiencies,^a Kinetic Isotope Effects ($k_{\text{H}}/k_{\text{D}}$), and Enthalpies of Reaction (kcal mol^{-1})^b for $\text{CN}^- + \text{RI}$ in the Gas Phase

Substrate (RI)	k_{exp}	Reaction Efficiency $k_{\text{exp}}/k_{\text{col}}$	$k_{\text{H}}/k_{\text{D}}^c$	$\text{S}_{\text{N}}2$ ΔH_{rxn}	E2 ΔH_{rxn}
CH_3I	12.8 ± 0.3	0.0574		-48.3	-
CD_3I	15.2 ± 0.7	0.0683	0.84 ± 0.03		
$\text{CH}_3\text{CH}_2\text{I}$	2.99 ± 0.02	0.0115		-48.6	-16.0
$\text{CH}_3\text{CD}_2\text{I}$	3.34 ± 0.09	0.0129	0.90 ± 0.03		
$\text{CD}_3\text{CH}_2\text{I}$	2.98 ± 0.06	0.0114	1.01 ± 0.02		
$\text{CD}_3\text{CD}_2\text{I}$	3.38 ± 0.07	0.0131	0.89 ± 0.02		
$(\text{CH}_3)_2\text{CHI}$	$<0.1^d$	<0.0004	-	-49.8	-17.8
$(\text{CH}_3)_3\text{CI}$	1.1 ± 0.1	0.004		-46.3	-17.2
$(\text{CD}_3)_3\text{CI}$	0.12 ± 0.01	0.0004	$>8^e$		

^a Efficiency is the ratio of the experimental rate constant to the collision rate constant calculated using parametrized trajectory collision theory.⁴⁰ ^b Enthalpies of reaction are calculated from thermochemical data.⁴¹ ^c Additional significant figures used in calculations are not reflected in rounded k_{exp} values. ^d The rate constant for CN^- reacting with isopropyl iodide is at the detection limits of the instrument. ^e This value is a lower limit without corrections for trace association products and mass discrimination.

this effect appears to be minimized in our KIE calculations due to the relatively small changes in the lowest frequencies upon isotopic substitution.

Results and Discussion

Gas Phase Reactions. The experimental rate constants, reaction efficiencies, and deuterium KIEs for the reactions of cyanide ion with alkyl iodides in the gas phase are given in Table 1. With the exception of the reaction of CN^- with isopropyl iodide, the reaction rate constants were within the detectable range of 10^{-9} to $10^{-12} \text{ cm}^3 \text{ molecule}^{-1} \text{ s}^{-1}$. The reaction efficiencies ($k_{\text{rxn}}/k_{\text{col}}$, where k_{col} is calculated using parametrized trajectory theory⁴⁰) are less than 7%; this low reactivity is consistent with the low proton affinity and delocalized nature of the anion. With efficiencies well below the collision-controlled limit, the KIEs are expected to reflect the intrinsic reactivity and differences in transition state structure. All enthalpies of reaction for the $\text{S}_{\text{N}}2$ pathways are at least 29 kcal mol^{-1} more exothermic than those for the E2 pathways. Although the E2 reactions are less exothermic, they are energetically accessible. In principle, the delocalization of charge density on CN^- allows the C or N atom to be the reactive site; however, thermochemical data⁴¹ indicate that attack of the neutral reactant by the carbon nucleophile is thermodynamically favored by approximately 18 kcal mol^{-1} based on heats of formation for CH_3CN versus CH_3NC and $\text{CH}_3\text{CH}_2\text{CN}$ versus $\text{CH}_3\text{CH}_2\text{NC}$. Therefore the alkyl cyanides were assumed to be the only products in our comparison of experimental and computational results.

In previous studies, reactivity trends and KIEs were utilized to assess the mechanistic behavior of the alkyl halides; different nucleophiles show significant differences in $\text{S}_{\text{N}}2$ and E2 branching fractions.^{13,42} "Typical" perdeutero KIE values for alkyl halides transition from inverse to normal as the amount of substitution on the α -carbon of the neutral reactant increases. Many ethyl halide reactions exhibit an increased efficiency when

compared with methyl halides. This has been attributed to either an increased stabilization of the $\text{S}_{\text{N}}2$ transition state and/or an E2 contribution to the reaction. Further substitution on the α carbon generates additional steric hindrance to the $\text{S}_{\text{N}}2$ reaction, which overcomes the $\text{S}_{\text{N}}2$ stabilizing electronic effects, leading to significant amounts of E2 reaction. Reactions of *tert*-butyl halides proceed exclusively by the E2 mechanism.¹³

An inverse $(k_{\text{H}}/k_{\text{D}})_{\alpha\text{-D}_3}$ of 0.84 ± 0.03 for reaction of CN^- with methyl iodide and a $(k_{\text{H}}/k_{\text{D}})_{\alpha\text{-D}_2}$ of 0.90 ± 0.03 for the reaction of CN^- with ethyl iodide are consistent with previously reported values for systems that proceed primarily or exclusively by an $\text{S}_{\text{N}}2$ mechanism.^{42,43} The unusually large KIE (>8) measured for the reaction of *tert*-butyl iodide with CN^- indicates that the reaction probably proceeds exclusively by an E2 mechanism. However unlike typical reaction systems, the reaction efficiency decreases from methyl to isopropyl and then increases for *tert*-butyl iodide. The observed decrease in rate constant from methyl to isopropyl shows the typical decrease in the $\text{S}_{\text{N}}2$ channel, but an unusually small increase in the E2 channel relative to previous results.^{13,17,42,43} The exceptionally large increase in the rate constant and efficiency from the isopropyl to the *tert*-butyl iodide reaction may be due to a significant release of steric strain in going to the transition state of the *tert*-butyl iodide reaction; i.e., *tert*-butyl iodide is especially strained due to the large iodine atom and the multiple methyl groups.

Condensed Phase Reactions. The rate constants expressed in both solution and gas phase units and the perdeutero KIEs for the $\text{S}_{\text{N}}2$ reaction between cyanide ion and methyl iodide in 40% $\text{CH}_3\text{OH}/60\%$ DMSO and ethyl iodide in 90% $\text{CH}_3\text{OH}/10\%$ DMSO, DMSO, and THF are presented in Table 2. All values are consistent with an $\text{S}_{\text{N}}2$ mechanism for the reaction.⁴⁴ The smaller (more inverse) KIE found for the methyl iodide-cyanide ion reaction in 40% $\text{CH}_3\text{OH}/60\%$ DMSO, Table 2, is expected if both substrates react by an $\text{S}_{\text{N}}2$ mechanism. These results suggest that the ethyl iodide-cyanide ion reaction in solution is an $\text{S}_{\text{N}}2$ process. This conclusion was confirmed by a gas chromatographic analysis of the neutral products; no ethylene, which would be produced in an E2 reaction, could be detected.¹²

The increase in the rate constant from $\text{CH}_3\text{OH}/\text{DMSO}$ to DMSO to THF is primarily due to the different solvation energies of the cyanide ion. The cyanide ion will be most stable in $\text{CH}_3\text{OH}/\text{DMSO}$ where it is solvated by hydrogen bonding, and the least stable (least solvated) in THF , the solvent with the lowest dielectric constant. The solvation energy of the transition state will increase from THF to DMSO to $\text{CH}_3\text{OH}/\text{DMSO}$. However, since the negative charge on the cyanide ion is dispersed (partially transferred to the developing iodide ion) in going to the transition state, the difference between the transition state energies in the different solvents will be smaller than that in the ground state. As a result, ΔH^\ddagger decreases (the rate constant increases) from $\text{CH}_3\text{OH}/\text{DMSO}$ to DMSO to THF (from protic to aprotic solvents) as depicted in Figure 1.

Comparison of Gas Phase and Solution Results. The transition states of the methyl and ethyl iodide reactions in solution and the gas phase were further probed using secondary α - and β -deuterium KIEs. These KIEs, measured in the condensed and gas phase, as well as the calculated branching fractions and KIEs are given in Table 3. It has been assumed that the solution

(40) Su, T.; Chesnavich, W. J. *J. Chem. Phys.* **1982**, *76*, 5183–5185.

(41) Linstrom, P. J., Mallard, W. G., Eds. *NIST Chemistry WebBook*; National Institute of Standards and Technology, NIST Standard Reference Database Number 69, Gaithersburg, MD 20899 (<http://webbook.nist.gov>; retrieved October 23, 2009).

(42) Gronert, S.; DePuy, C. H.; Bierbaum, V. M. *J. Am. Chem. Soc.* **1991**, *113*, 4009–4010.

(43) Bierbaum, V. M.; Grabowski, J. J.; DePuy, C. H. *J. Phys. Chem.* **1984**, *88*, 1389–1393.

(44) Westaway, K. C.; Waszczylo, Z. *Can. J. Chem.* **1982**, *60*, 2500–2520.

Table 2. Rate Constants and Perdeutero KIEs (k_H/k_D) for the $\text{CN}^- + \text{CH}_3\text{I}$ and $\text{CN}^- + \text{CH}_3\text{CH}_2\text{I}$ Reactions in the Protic to Aprotic Solvent Series

Solvent (Temp)	Reaction	k_H ($\text{M}^{-1} \text{s}^{-1}$)	k_H ($\text{cm}^3 \text{s}^{-1}$)	Perdeutero k_H/k_D
40% $\text{CH}_3\text{OH}/$ 60% DMSO (20 °C)	$\text{CN}^- + \text{CH}_3\text{I}$	$5.63 (\pm 0.02) \times 10^{-2}$	9.34×10^{-23}	0.902 ± 0.004
90% $\text{CH}_3\text{OH}/$ 10% DMSO (30 °C)	$\text{CN}^- + \text{CH}_3\text{CH}_2\text{I}$	$5.84 (\pm 0.13) \times 10^{-5}$	9.69×10^{-26}	1.02 ± 0.03
DMSO (20 °C)	$\text{CN}^- + \text{CH}_3\text{CH}_2\text{I}$	0.2075 ± 0.004	3.44×10^{-22}	1.044 ± 0.002
THF (0 °C)	$\text{CN}^- + \text{CH}_3\text{CH}_2\text{I}$	0.4051 ± 0.0007	6.72×10^{-22}	1.062 ± 0.003

Table 3. A Comparison of Experimental and Theoretical^a Deuterium KIEs for the $\text{CN}^- + \text{CH}_3\text{I}$ and $\text{CN}^- + \text{CH}_3\text{CH}_2\text{I}$ Reactions in the Gas Phase^b and in Solution^c

Reaction Phase	$\text{CN}^- + \text{CH}_3\text{I}$			$\text{CN}^- + \text{CH}_3\text{CH}_2\text{I}$			
	$(k_H/k_D)_{\alpha\text{-D3}}$	$(k_H/k_D)_{\text{D5}}$	Corrected $(k_H/k_D)_{\text{D5}}$ (20 °C)	$(k_H/k_D)_{\alpha\text{-D2}}$	Corrected $(k_H/k_D)_{\alpha\text{-D2}}$ (20 °C)	$(k_H/k_D)_{\beta\text{-D3}}$	Corrected $(k_H/k_D)_{\beta\text{-D3}}$ (20 °C)
40% $\text{CH}_3\text{OH}/$ 60% DMSO	0.902 ± 0.004^d	—	—	—	—	—	—
90% $\text{CH}_3\text{OH}/$ 10% DMSO	—	1.02 ± 0.03^e	1.03 ± 0.04	1.015 ± 0.02^e	1.03 ± 0.03	1.005^g	1.00^g
DMSO	—	1.044 ± 0.002^d	1.044 ± 0.002	1.032 ± 0.004^d	1.032 ± 0.004	1.012^g	1.012^g
THF	—	1.062 ± 0.003^f	1.04 ± 0.02	1.040 ± 0.003^f	1.02 ± 0.02	1.021^g	1.02^g
Gas phase	0.84 ± 0.03	0.89 ± 0.02		0.90 ± 0.03		1.01 ± 0.02	
Theoretical $\text{S}_{\text{N}}2$							
Gas phase	0.83	0.89		0.91		0.97	
THF	---	1.087		1.059		1.028	
Theoretical E2							
Gas phase	---	8.4		1.1		7.8	

^a Theoretical $\text{S}_{\text{N}}2$ and E2 KIEs used conventional transition state theory and ΔG^\ddagger at the MP2 level of theory with the 6-311++g(2d,p) basis set for C, N, and H and the LanL2DZ effective core potential for I at 298 K. ^b The error in the gas phase KIEs is 1 standard deviation of at least three measurements. Experiments conducted at 298 K. ^c The error in the solution KIEs is $1/k_{\text{D}}[(\Delta k_{\text{H}})^2 + (k_{\text{H}}/k_{\text{D}})^2 \times (\Delta k_{\text{D}})^2]^{1/2}$, where Δk_{H} and Δk_{D} are the standard deviations for the average rate constants for the undeuterated and deuterated substrates, respectively. ^d Experiments conducted at 20 °C. ^e Experiments conducted at 30 °C. ^f Experiments conducted at 0 °C. ^g The $(k_{\text{H}}/k_{\text{D}})_{\beta\text{-D3}}$ /corrected $(k_{\text{H}}/k_{\text{D}})_{\beta\text{-D3}}$ was calculated by dividing the experimental/corrected experimental $(k_{\text{H}}/k_{\text{D}})_{\text{D5}}$ by the experimental/corrected experimental $(k_{\text{H}}/k_{\text{D}})_{\alpha\text{-D2}}$.

perdeutero KIE for the ethyl iodide reaction is the product of the $(k_{\text{H}}/k_{\text{D}})_{\beta\text{-D3}}$ and $(k_{\text{H}}/k_{\text{D}})_{\alpha\text{-D2}}$:

$$\frac{k_{\text{CN}^- + \text{CH}_3\text{CH}_2\text{I}}}{k_{\text{CN}^- + \text{CD}_3\text{CD}_2\text{I}}} = \frac{k_{\text{CN}^- + \text{CH}_3\text{CH}_2\text{I}}}{k_{\text{CN}^- + \text{CD}_3\text{CH}_2\text{I}}} \times \frac{k_{\text{CN}^- + \text{CH}_3\text{CH}_2\text{I}}}{k_{\text{CN}^- + \text{CH}_3\text{CD}_2\text{I}}} = (k_{\text{H}}/k_{\text{D}})_{\beta\text{-D3}} \times (k_{\text{H}}/k_{\text{D}})_{\alpha\text{-D2}}$$

Because the $(k_{\text{H}}/k_{\text{D}})_{\beta\text{-D3}}$ values for the reactions in solution were expected to be near unity, they were calculated from this relationship rather than experimentally measured. While the current gas phase data as well as our computational results support the use of this multiplicative technique, other gas phase results^{29,45} indicate this relationship may only be an approximation rather than a rigid equality. To accommodate the inexact nature of the relationship, no error bars have been given for the $(k_{\text{H}}/k_{\text{D}})_{\beta\text{-D3}}$ values in solution.

Because the rate of the ethyl iodide–cyanide ion reaction changed by a factor of 10^4 when the solvent was changed from $\text{CH}_3\text{OH}/\text{DMSO}$ to THF, the rate constants and the KIEs could not be measured at the same temperature in the three solvents, Table 3. To accurately compare the KIEs in the different solvents, a temperature correction for the KIE was needed. This was possible for the $(k_{\text{H}}/k_{\text{D}})_{\alpha\text{-D2}}$ values. The average temperature dependence of $(k_{\text{H}}/k_{\text{D}})_{\alpha\text{-D2}}$ from 34 reactions in three different laboratories^{44,46,47} was $1.0 (\pm 1.0) \times 10^{-3}/^\circ\text{C}$. Applying this correction to the $(k_{\text{H}}/k_{\text{D}})_{\alpha\text{-D2}}$ in Table 3 gives the best estimate

of the $(k_{\text{H}}/k_{\text{D}})_{\alpha\text{-D2}}$ for the $\text{S}_{\text{N}}2$ reaction between the cyanide ion and ethyl iodide in the three solvents at 20 °C, column 6, Table 3. Although no temperature dependence could be found for the $(k_{\text{H}}/k_{\text{D}})_{\beta\text{-D3}}$ or $(k_{\text{H}}/k_{\text{D}})_{\text{D5}}$ KIEs, a comparison of the magnitude of these KIEs suggests a relatively small correction factor for the $(k_{\text{H}}/k_{\text{D}})_{\beta\text{-D3}}$. Therefore, using the single component $(k_{\text{H}}/k_{\text{D}})_{\alpha\text{-D2}}$ correction should provide a good estimate of the actual $(k_{\text{H}}/k_{\text{D}})_{\text{D5}}$ values in solution; the corrected $(k_{\text{H}}/k_{\text{D}})_{\text{D5}}$ values at 20 °C are given in column 4, Table 3.

Computations were carried out to provide additional insight into the experimental results. The MP2³⁴ level of theory with the 6-311++g(2d,p) basis set for C, N, and H and the LanL2DZ effective core potential for I correctly predicted the observed $(k_{\text{H}}/k_{\text{D}})_{\alpha\text{-D3}}$ for the methyl iodide–cyanide ion reaction that can only occur by the $\text{S}_{\text{N}}2$ mechanism, i.e., the computational $(k_{\text{H}}/k_{\text{D}})_{\alpha\text{-D3}}$ of 0.83 found for the $\text{CN}^- + \text{CH}_3\text{I}$ reaction is in excellent agreement with the experimental gas phase $(k_{\text{H}}/k_{\text{D}})_{\alpha\text{-D3}}$ of 0.84 ± 0.03 . Therefore, this level of theory was used in all subsequent calculations. Solvent calculations were conducted at the same level of theory employing the polarizable continuum model with a THF dielectric parameter for the ethyl iodide reactions. Since standard dielectric parameters for mixed solvents are not available in the Gaussian database, condensed phase KIE calculations for the $\text{CN}^- + \text{CH}_3\text{I}$ reaction were not carried out. Consistent with experimental data no transition state structures were found for the E2 reactions in the condensed phase. The direction of the calculated KIEs is in good agreement

(45) Villano, S. M.; Eyet, N.; Lineberger, W. C.; Bierbaum, V. M. *J. Am. Chem. Soc.* **2009**, *131*, 8227–8233.

(46) Koshy, K. M.; Robertson, R. E. *J. Am. Chem. Soc.* **1974**, *96*, 914–916.

(47) Shiner, V. J., Jr.; Dowd, W.; Fisher, R. D.; Hartshorn, S. R.; Kessick, M. A.; Milakof, L.; Rapp, M. W. *J. Am. Chem. Soc.* **1969**, *91*, 4838–4939.

with experimental data. While the consistency of the calculated KIEs for both the gas phase and THF solvent provides support for our methodology and use of relative KIEs to infer branching fractions, the qualitative predictions are considered more reliable than quantitative interpretations.

The theoretical KIE for the methyl iodide–cyanide ion reaction (0.83) is significantly smaller (more inverse) than the theoretical S_N2 $(k_H/k_D)_{\alpha-D2}$ for the gas phase ethyl iodide–cyanide ion reaction (0.91). This larger (less inverse) KIE for ethyl iodide reflects the additional stabilization of the transition state by the polarizable alkyl group,^{13,15,17} the looser transition states found for the S_N2 reactions of ethyl substrates,⁴⁸ and the fact that this isotope effect is now due to only two hydrogens rather than three as in the methyl iodide case. The large magnitude of the E2 $(k_H/k_D)_{D5}$ calculated for the gas phase ethyl iodide–cyanide reaction (8.4) arises from a substantial primary (7.8) and a smaller secondary (1.1) KIE. It is consistent with the large primary hydrogen–deuterium KIE observed for the E2 reaction between the cyanide ion and *tert*-butyl iodide (>8). Although the calculated KIEs for the E2 reaction are large compared to those typically found for E2 reactions (KIE = 2–7), they are in good agreement with the KIEs found experimentally and computationally by Gronert et al.⁴⁹ for E2 reactions in the gas phase.

Our transition state theory calculations predict the ethyl iodide–cyanide ion reaction to be 99% S_N2 and 1% E2. The presence of a small amount of E2 elimination in the gas phase reaction is consistent within the error range of a comparison of experimental and computational KIEs. Consider first the gas phase experimental $(k_H/k_D)_{\beta-D3}$ value of 1.01, which exceeds the computational S_N2 value (KIE = 0.97). A simple calculation, detailed in the Supporting Information, shows that this experimental value can be reproduced by a 4% contribution of the E2 channel (KIE = 7.8). While the experimental $(k_H/k_D)_{\alpha-D2}$ and $(k_H/k_D)_{D5}$ values suggest no contribution from the E2 channel, the error bars on these values definitely allow a small amount of elimination pathway. Thus, both the transition state theory calculations and the experimental KIEs suggest there is a small amount of E2 pathway in the gas phase reaction, whereas there is none in solution. The E2 channel probably competes more effectively with the S_N2 channel in the gas phase because the solvation energy decreases the basicity of the anion in solution.

An examination of the $(k_H/k_D)_{D5}$ and $(k_H/k_D)_{\alpha-D2}$ values at 20 °C in columns 4 and 6 of Table 3 shows that neither KIE is affected significantly by the change in solvent from CH₃OH/DMSO to THF even though the rate constant changes by approximately 10⁴. This indicates that the structure of the S_N2 transition state is not affected significantly by a change in solvent. This result is in agreement with Westaway's "Solvation Rule for S_N2 Reactions,"⁵⁰ which predicts that there will be little or no change in transition state structure in a Type I S_N2 reaction (where the nucleophile and the leaving group have the same charge, as is the case for CN[−] and I[−]) when the solvent is changed. It is worth noting that there was only a slight tightening of transition state structure when the solvent was

changed from DMSO to THF for the Type I S_N2 reaction between ethyl chloride and the cyanide ion.⁵¹

A comparison of the $(k_H/k_D)_{\alpha-D2}$ and the $(k_H/k_D)_{D5}$ values for the gas phase and solution results show that the KIEs in the gas phase are significantly smaller (more inverse) than those in solution. For example, the $(k_H/k_D)_{\alpha-D2}$ values for the gas phase and solution are 0.84 and 0.902 for the methyl iodide reaction and 0.90 and 1.03 for the ethyl iodide reaction, respectively. The same trend is observed in the $(k_H/k_D)_{D5}$ results for the ethyl iodide reaction, i.e., 0.89 in the gas phase and 1.04 in solution. The smaller KIEs indicate a considerably tighter transition state in the gas phase.^{48,52–54} Although the calculations in THF using the polarizable continuum model correctly predict the larger secondary alpha, beta, and perdeutero KIEs for the ethyl iodide–cyanide ion reaction that are consistent with a looser transition state in solution, there is poorer agreement between experiment and theory than for the gas phase analogues. Comparison of transition state structures from our theoretical gas-phase and the polarizable continuum model calculations displays a longer C_α - I bond and a shorter NC - C_α bond for the condensed phase (see Supporting Information). Although the PCM model only accounts for electrostatic solute–solvent interactions, it is possible that solvent effects advance the CN[−] + CH₃CH₂I reaction along the reaction coordinate toward a more product-like transition state. However, experimental KIEs from studies⁵¹ for the ethyl chloride–cyanide ion S_N2 reaction in DMSO and THF suggest that both the NC - C_α and the C_α - Cl bonds are shorter in the transition state for the less polar (less solvating) solvent (THF). Clearly further computational studies are warranted.

It is important to note that Westaway's Solvation Rule, which holds in solution very well, fails the ultimate test because the transition state changes significantly on going to the gas phase. The tighter transition state in the gas phase probably occurs because the electrostatic attraction between the partial negative charges on the cyanide and iodide ions and the partial positive charge on the α carbon is much more important in determining transition state structure in the gas phase than when the charges on the cyanide and iodide ions are reduced by solvation in solution. The tighter transition state in the gas phase is evident in the 7% difference in our $(k_H/k_D)_{\alpha-D3}$ values for the gas phase and solution (0.84 and 0.902, respectively) for the methyl iodide reaction. This trend is even more evident in the ethyl iodide reaction; i.e., the $(k_H/k_D)_{\alpha-D2}$ and $(k_H/k_D)_{D5}$ values in the gas phase and in solution differ by 15% and 17%, respectively.

The significant difference between the KIEs and the transition state structures in the gas phase and solution was initially troubling since the use of THF was expected to approach gas phase conditions. However, Bogdanov and McMahon⁵⁵ have shown that even though THF has a low dielectric constant ($\kappa = 7$), it is far from the gas phase limit. Figure 2 shows their computed values for ΔE^\ddagger for the Cl[−] + CH₃Cl reaction as a function of the dielectric constant of the solvent. Changing the solvent from CH₃OH/DMSO to THF for the S_N2 reaction between methyl chloride and chloride ion would reduce ΔE^\ddagger

(48) Poirier, R. A.; Wang, Y. L.; Westaway, K. C. *J. Am. Chem. Soc.* **1994**, *116*, 2526–2533.

(49) Gronert, S.; Fagin, A. E.; Wong, L. *J. Am. Chem. Soc.* **2007**, *129*, 5330–5331.

(50) Westaway, K. C. *Can. J. Chem.* **1978**, *56*, 2691–2699.

(51) Fang, Y. R.; MacMillar, S.; Eriksson, J.; Kolodziejska-Huben, M.; Dybala-Defratyka, A.; Paneth, P.; Matsson, O.; Westaway, K. C. *J. Org. Chem.* **2006**, *71*, 4742–4747.

(52) Kato, S.; Davico, G. E.; Lee, H. S.; DePuy, C. H.; Bierbaum, V. M. *Int. J. Mass Spectrom.* **2001**, *210*, 223–229.

(53) Glad, S. S.; Jensen, F. *J. Am. Chem. Soc.* **1997**, *119*, 227–232.

(54) Westaway, K. C. *Adv. Phys. Org. Chem.* **2006**, *41*, 217–273.

(55) Bogdanov, B.; McMahon, T. B. *Int. J. Mass Spectrom.* **2005**, *241*, 205–223.

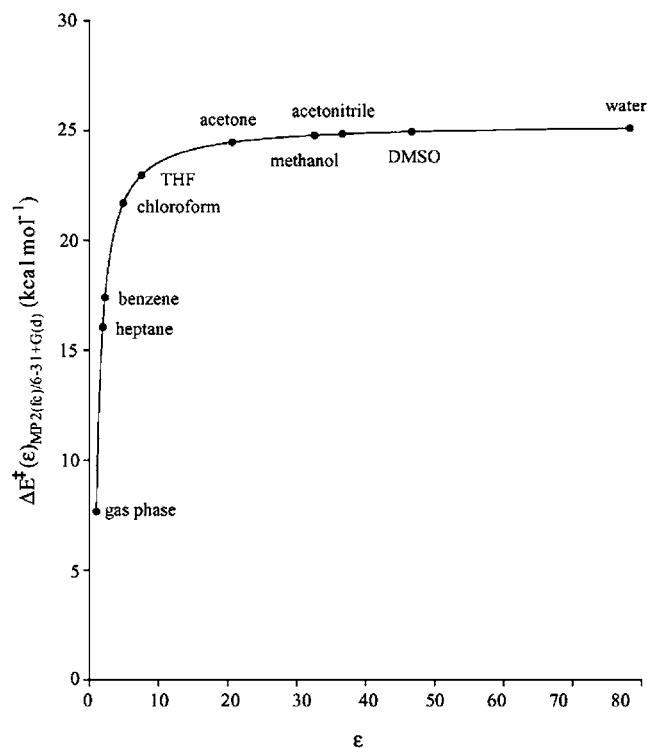


Figure 2. Plot of the dielectric constant (ϵ) vs the activation energy for the $\text{Cl}^- + \text{CH}_3\text{Cl}$ $\text{S}_{\text{N}}2$ reaction, $\Delta E^\ddagger(\epsilon)_{\text{MP2}(\text{fc})/6-31+\text{G}(\text{d})}$, in various solvents.⁵⁶

by only 2 kcal mol⁻¹; in contrast, going from CH₃OH/DMSO to the gas phase would reduce ΔE^\ddagger by over 17 kcal mol⁻¹. Given the large difference in ΔE^\ddagger between the gas phase and THF (approximately 15 kcal mol⁻¹) the observation of a significantly tighter transition state in the gas phase is a reasonable result. The curve in Figure 2 also explains why the reaction is between 10¹¹ and 10¹⁵ times faster in the gas phase than in solution (see Tables 1 and 2 and Figure 1). Finally, the magnitudes of the electrostatic attraction between the partial negative charges on the nucleophiles in the transition state (cyanide ion and iodide ion) and the partial positive charge on the α carbon are much larger in the gas phase than in THF where solvation will reduce the electrostatic attraction between the ions in the transition state. This greater electrostatic attraction in the gas phase transition

state is likely responsible for the tighter transition state and more inverse KIEs observed in the gas phase.⁴⁹

Conclusions

The reaction of a cyanide ion with ethyl iodide provides an ideal system for comparing gas and solution data. Both gas phase and solution reactions are dominated by the $\text{S}_{\text{N}}2$ pathway and have reactivities that are measurable and sensitive to isotopic substitution. In addition, the system is a Type I $\text{S}_{\text{N}}2$ reaction where changes in solvent are predicted to have minimal or no effect on transition state structure and the KIEs. A direct comparison of KIEs between the gas phase and solution showed that the KIEs in the gas phase are significantly smaller (more inverse) than those in solution. This result indicates that the transition state is significantly tighter in the gas phase. Thus, although the “Solvation Rule for $\text{S}_{\text{N}}2$ Reactions” has successfully predicted the change in transition state structure for a wide range of $\text{S}_{\text{N}}2$ reactions in solution,⁵⁴ it fails the ultimate test of predicting the effect of removing the solvent completely. The tighter transition state in the gas phase is primarily attributed to bond changes due to the greater electrostatic forces between the partial negative charges on iodide and cyanide ions and the partial positive charge on the α carbon in the gas phase.

Acknowledgment. The authors gratefully acknowledge support of this work by the National Science Foundation (CHE 0647088), the AFOSR (FA9550-09-1-0046), and a grant from the Natural Sciences and Engineering Research Council of Canada (NSERC). J.M.G. respectfully acknowledges the sponsorship and support of the Air Force Institute of Technology. The computational work was supported by an allocation through the TeraGrid Advanced Support Program. We appreciate the insightful discussions with Professor Charles H. DePuy, Dr. Zhibo Yang, and Professor Eric Patterson.

Supporting Information Available: Complete Gaussian reference, calculation of the E2 branching fraction, and computational geometries, harmonic frequencies, and rotational constants are provided. This material is available free of charge via the Internet at <http://pubs.acs.org>.

JA909399U

(56) Reprinted from Bogdanov, B.; McMahon, T. B. *Int. J. Mass Spectrom.* **2005**, *241*, 205–223, Copyright (2005), with permission from Elsevier.